Electronic Supplementary Material (ESI) for Chemical Science.
This journal is © The Royal Society of Chemistry 2021

Electronic Supplementary Information

Integration of exonuclease III-powered three-dimensional DNA walker with single-molecule detection for multiple initiator caspases assay

Meng Liu,[‡a] Rui Xu,[‡a] Wenjing Liu,[‡b] Jian-Ge Qiu,*[b] Yan Wang,*[a] Fei Ma,*[c] Chun-yang Zhang*[a]

[a] College of Chemistry, Chemical Engineering and Materials Science, Collaborative Innovation Center of Functionalized Probes for Chemical Imaging in Universities of Shandong, Key Laboratory of Molecular and Nano Probes, Ministry of Education, Shandong Provincial Key Laboratory of Clean Production of Fine Chemicals, Shandong Normal University, Jinan 250014, China.

[b] Academy of Medical Sciences, the Affiliated Cancer Hospital of Zhengzhou University, Zhengzhou University, Zhengzhou, 450000, China.

[c] School of Chemistry and Chemical Engineering, Southeast University, Nanjing, 211189, China.

*Correspondence authors. Tel.: +86 0531-86186033; Fax: +86 0531-82615258. E-mail: cyzhang@sdnu.edu.cn, jiangeqiu@zzu.edu.cn, fagong@sdu.edu.cn, fei@seu.edu.cn.

[‡] These authors contributed equally.

1. Mechanism of caspase cleavage.

The caspase cleavage involves two steps: (1) identification of specific peptide site and (2) hydrolysis of the peptide bond. The specifical recognition tetrapeptide sequence is IETD for caspase-8 (Fig. S1A) and LEHD for caspase-9 (Fig. S1B). After identification, caspases will cleave the peptide substrates at the peptide bond between the Asp and Gly residues, respectively. As a result, the cleaved peptide-DNA probe can be released.

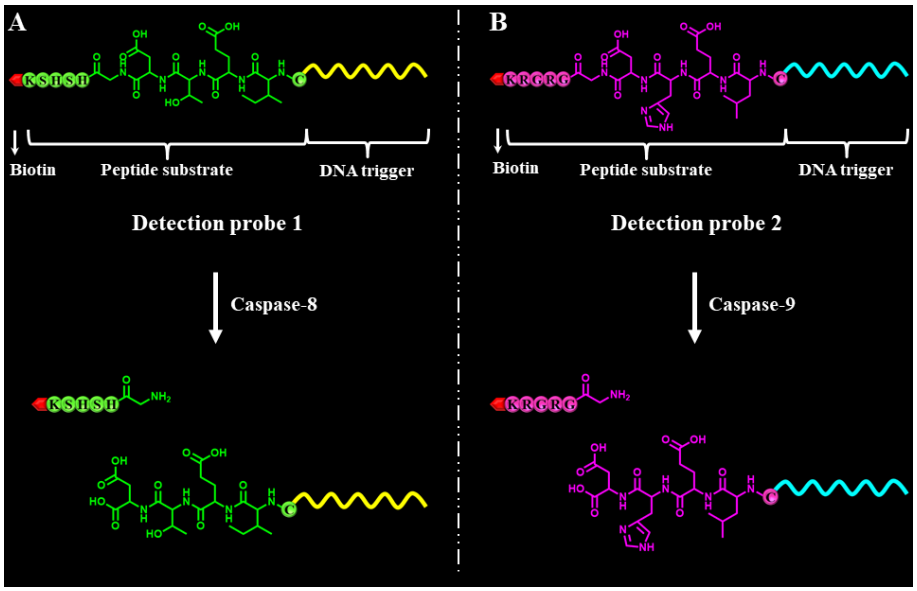

Fig. S1 Mechanism of the caspase cleavage of detection probes. The peptide substrates are shown in green in detection probe 1 and magenta in detection probe 2, respectively. The DNA triggers are shown in yellow in detection probe 1 and cyan in detection probe 2, respectively.

2. Characterization of signal probes-functioned AuNPs and the number of signal probes per AuNP.

To verify the signal probes bound to the surface of AuNPs through the covalent S-Au bond, we measured the UV absorption spectra of the signal probe-functioned AuNPs. As shown in Fig. S2, only an absorption peak at 520 nm is detected in the presence of AuNPs (black curve), and the

absorption peaks at 260 nm, 650 nm (Fig. S2A, blue curve) are observed in the presence of Cy5-labeled signal probe 1, and the absorption peaks at 260 nm and 600 nm (Fig. S2B, magenta curve) are observed in the presence of Texas Red-labeled signal probe 2. In contrast, because of the increase of the AuNP diameter induced by the linkage of DNA ligands to the AuNPs, a slight shift in the surface plasmon resonance peak from 520 nm to 524 nm for the signal probe 1-modified AuNPs (Fig. S2A, red curve) and from 520 nm to 525 nm for the signal probe 2-modified AuNPs (Fig. S2B, green curve) is observed, respectively, indicating that the signal probes are successfully bound to the AuNPs.

The number of signal probes per AuNP is calculated by measuring AuNPs and signal probes (2.35 nmol), respectively. Because 1 mL of AuNPs (5.70×10^{12} particles/mL, 9.40 nM) is used to bind the signal probes and the concentration of signal probes modified on the AuNP surface is determined to be 28.25 ± 0.29 μM for signal probe 1 and 28.33 ± 0.23 μM for signal probe 2 in the final volume of 40 μL, the number of signal probes per AuNP is estimated to be 120 ± 1 for both signal probe 1 and signal probe 2.

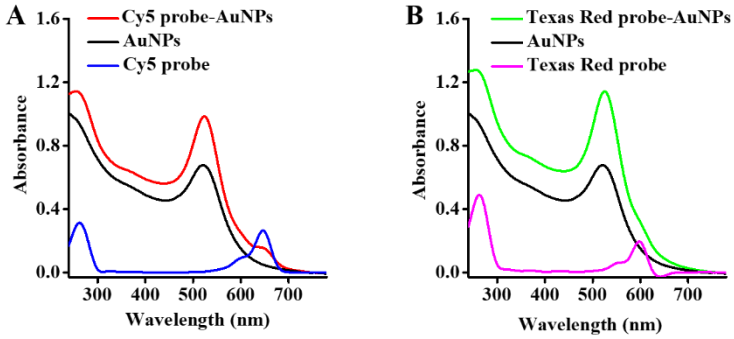

Fig. S2 (A) UV-Vis absorption spectra of AuNPs (black color), Cy5-labeled signal probe 1 (10 μM, blue color), and signal probe 1-modified AuNPs (red color). (B) UV-Vis absorption spectra of AuNPs (black color), Texas Red-labeled signal probe 2 (10 μM, magenta color), and signal probe 2-modified AuNPs (green color).

3. Single-molecule stepwise-photobleaching trajectories.

We performed the single molecule photobleaching experiment to verify single-molecule detection. The samples were continuously excited by a 640 nm laser for Cy5 dye molecules and a 561 nm laser for Texas Red dye molecules, and the fluorescent images were recorded at a high-frequency with an exposure time of 400 ms. Totally fifty frames were acquired and subjected to data analysis. As shown in Fig. S3, both the Cy5 and Texas Red fluorescence spots exhibit single-step photobleaching, suggesting that the individual spot is originated from single dye molecule.

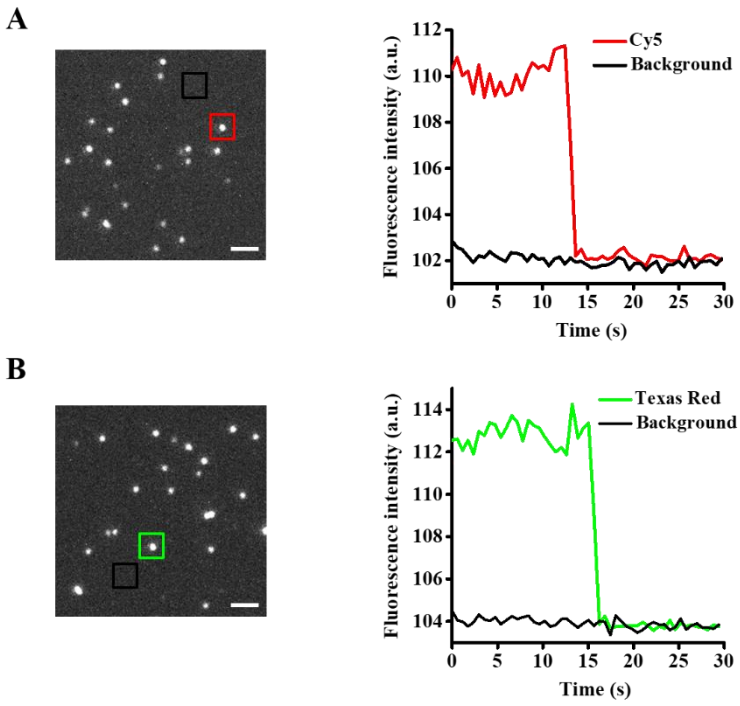

Fig. S3 Intensity traces over time showing one photobleaching step for individual Cy5 (A) and Texas Red (B) fluorescence spots. The fluorescence images prior to photobleaching process are shown in the left panel. The scale bar is 2 μm.

4. Optimization of experimental conditions.

To achieve the best assay performance, we optimized the temperature and incubation time of caspase

cleavage reaction, the number of signal probes per AuNP, and the amount of Exo III. We investigated the effect of temperature upon the caspase cleavage reaction. As shown in Fig. S4A, the Cy5 counts improve with the increase of reaction temperature from 30 to 37 °C, followed by the decrease beyond the temperature of 37 °C. Similarly, the Texas Red counts improve with the increase of reaction temperature from 30 to 37 °C, followed by the decrease beyond the temperature of 37 °C. Thus, 37 °C is used as the caspase-medicated cleavage reaction temperature in the subsequent researches.

We further investigated the effect of caspase reaction time upon the assay performance. As shown in Fig. S4B, the Cy5 counts improve with the reaction time from 10 to 60 min, and reach a plateau at 60 min. The Texas Red counts enhance with the reaction time from 10 to 60 min, and reach a plateau at 60 min, too. This can be explained by either the complete loss of caspase activity or the consumption of all available peptide substrates. Thus, the caspase incubation time of 60 min is used in the subsequent researches.

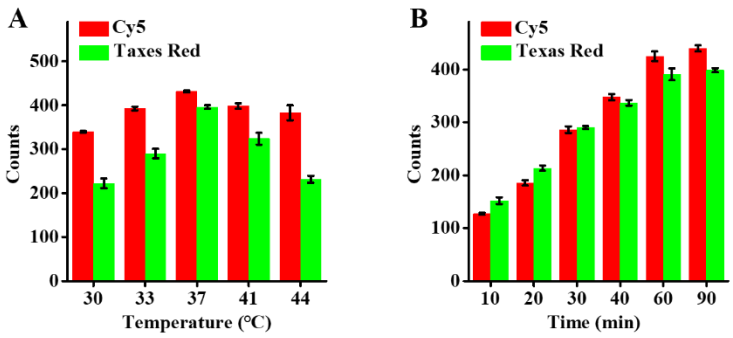

Fig. S4 (A) Variance of Cy5 counts in response to different temperature of the caspase-mediated cleavage reaction in the presence of 0.025 U/μL caspase-8 (red column), and variance of Texas Red counts in response to different temperature of the caspase-mediated reaction in the presence of 0.025 U/μL caspase-9 (green column). (B) Variance of Cy5 counts in response to different incubation time of the caspase-mediated cleavage reaction in the presence of 0.025 U/μL caspase-8 (red column),

and variance of Texas Red counts in response to different incubation time of the caspase-mediated cleavage reaction in the presence of 0.025 U/μL caspase-9 (green column). Error bars represent the standard deviation of three experiments.

The surface density of DNA on AuNPs can change the DNA conformation on AuNPs. To achieve the best performance of the Exo III-powered 3D DNA walker, we optimized the number of signal probes per AuNP and the amount of Exo III. As shown in Fig. S5A, different amounts of Cy5-labeled signal probe 1 were mixed with a fixed amount of AuNP (1 mL) to obtain the signal probe 1@AuNP with different numbers of signal probe 1 per AuNP. We investigated the effect of the signal probe 1 per AuNP upon the assay performance by monitoring the variance of the F/F_0 value with the number of signal probe 1 per AuNP, where F_0 and F are the Cy5 fluorescence intensity in the absence and presence of 0.025 U/μL caspase-8, respectively. The F/F_0 value enhances with the increasing number of signal probe 1 per AuNP from 30 to 120, followed by the decrease beyond the number of 120. Similarly, different amounts of Texas Red-labeled signal probe 2 were mixed with a fixed amount of AuNP (1 mL) to obtain the signal probe 2@AuNP with different numbers of signal probe 2 per AuNP. We investigated the effect of the signal probe 2 per AuNP upon the assay performance by monitoring the variance of the F/F_0 value with the number of signal probe 2 per AuNP, where F_0 and F are the Texas Red fluorescence intensity in the absence and presence of 0.025 U/μL caspase-9, respectively. The F/F_0 value enhances with the increasing number of signal probe 2 per AuNP from 30 to 120, followed by the decrease beyond the number of 120. The reason for this phenomenon may be that the surface conformation of DNA stops to change beyond the number of 120 and the higher density brings a larger steric hindrance for Exo III digestion. Therefore, the

number of signal probe 2 per AuNP of 120 is used in the subsequent researches. As shown in Fig. S5B, the Cy5 and Texas Red counts enhance with the increasing amounts of Exo III from 0.05 to 0.5 U, and it tends to saturate beyond the amount of 0.5 U due to the exhaustion of signal probes. Therefore, 0.5 U of Exo III is used in the subsequent researches.

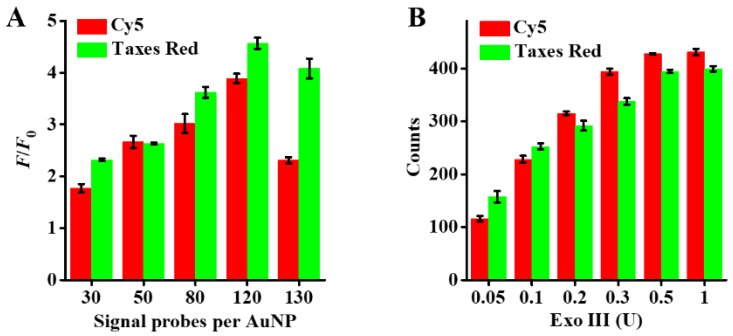

Fig. S5 (A) Value of F/F_0 with the number of Cy5-labeled signal probe 1 per AuNP (red column) and Texas Red-labeled signal probe 2 per AuNP (green column), respectively. F and F_0 are the fluorescence intensity in the presence and absence of caspase-8 and caspase-9, respectively. The 0.025 U/μL caspase-8 and 0.025 U/μL caspase-9 were used in the experiments. (B) Variance of Cy5 counts with the amounts of Exo III in the presence of 0.025 U/μL caspase-8 (red column), and variance of Texas Red counts with the amounts of Exo III in the presence of 0.025 U/μL caspase-9 (green column). Error bars represent the standard deviation of three experiments.

5. Inhibition effect of antibody.

To evaluate the inhibition effect of antibody on caspase, we measured the fluorescent counts in the presence of target caspase and different concentrations of caspase antibody. As shown in Fig. S6A, the Cy5 counts decrease with the increasing concentration of anti-caspase-8 antibody from 0 to 3.75 mg/L, and reaches a level comparable to that of the control group without caspase-8 beyond the concentration of 3.75 mg/L, indicating the complete inhibition of caspase-8 activity by anti-caspase-

8 antibody. Moreover, the Texas Red counts decrease with the increasing concentration of anti-caspase-9 antibody from 0 to 4.85 mg/L (Fig. S6B), and reaches a level comparable to that of the control group without caspase-9 beyond the concentration of 4.85 mg/L, indicating the complete inhibition of caspase-9 activity by anti-caspase-9 antibody.

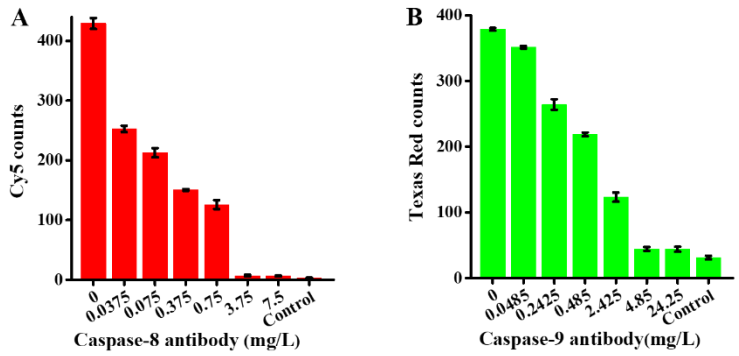

Fig. S6 (A) Variance of Cy5 counts in response to different concentrations of caspase-8 antibody in the presence of 0.025 U/μL caspase-8 and absence of caspase-8 (control), respectively. (B) Variance of Texas Red counts in response to different concentrations of caspase-9 antibody in the presence of 0.025 U/μL caspase-9 and absence of caspase-9 (control), respectively. Error bars represent the standard deviation of three experiments.

6. Comparison with other caspases assays.

Table S1. Comparison of current method with the reported methods for caspase assay.

Target	Strategy	Assay time*	Signal amplification	LOD	Ref.
Caspase-8, caspase-9	Exo III-powered 3D DNA walker and single-molecule detection	4.5 h	yes	2.08×10^{-6} U/μL (or 7.51 pM) for caspase-8, 1.71×10^{-6} U/μL for caspase-9 (92.37 pM)	this method
Caspase-8	Thiol-ene click reaction-based spatially resolved imaging	>21 h	no	10 pM	1
Caspase-3, caspase-8	Conjugated polymer-based real-time fluorescence	4 h 15 min for caspase-3, 1.5 h for caspase-8	no	0.1 U/mL for caspase 3, 0.2 U/mL for caspase 8	2
Caspase-8	High-performance liquid chromatography (HPLC) with N-terminal Ser-containing peptides -based fluorescence reaction	99 min	no	2 U (4.3 nM) for caspase-3, 2.5 U (3.3 nM) for caspase-8	3
Caspase-9	Peptide-functionalized upconversion nanoparticles-based FRET	21 h 50 min	no	0.068 U/mL	4
Cytochrome c, caspase-9	Antibody-based real-time and in situ electrochemical detection	5 h 10 min	no	0.08 ± 0.02 μM	5

*Assay time includes the time for both probe preparation and activity detection.

7. References

1. W. Liu, S.-J. Liu, Y.-Q. Kuang, F.-Y. Luo and J.-H. Jiang, *Anal. Chem.*, 2016, **88**, 7867-7872.

2. Y. Xie, R. Zhao, Y. Tan, X. Zhang, F. Liu, Y. Jiang and C. Tan, *ACS Appl. Mater. Interfaces*, 2012, **4**, 405-410.

3. M. S. Rahman, T. Kabashima, H. Yasmin, T. Shibata and M. Kai, *Anal. Biochem.*, 2013, **433**, 79-85.

4. L. Liu, H. Zhang, Z. Wang and D. Song, *Biosens. Bioelectron.*, 2019, **141**, 111403.

5. Q. Wen, X. Zhang, J. Cai and P.-H. Yang, *Analyst*, 2014, **139**, 2499-2506.